A Scalable MOS Device Substrate Resistance Model for RF and Microwave Circuit Simulation

by Mohan Vamsi Dunga

Research Project

Submitted to the Department of Electrical Engineering and Computer Sciences, University of California at Berkeley, in partial satisfaction of the requirements for the degree of **Master of Science, Plan II**.

Approval for the Report and Comprehensive Examination:

Committee:

Prof. Ali Niknejad
Research Advisor

Date

* * * * * *

Prof. Chenming Hu
Second Reader

Date

Contents

Chapter 1

Introduction

Recent years have seen an enormous growth in RF circuit applications. Until recently, most RF circuits and systems have been implemented with either compound semiconductor transistors, such as GaAs MESFETs, HEMTs and HBTs or silicon BJTs. However, the microwave properties of silicon MOSFETs were inferior to those of other high-frequency transistors. The continuous down-scaling of MOSFETs into deep-submicron dimensions has led to transistors with very high unity-gain frequencies making MOSFETs attractive for RF applications [1] [2] [3]. CMOS processes can reach 100-GHz f_t making them increasingly attractive for high-frequency analog electronics and wireless communications.

RF circuit design has severe constraints on power consumption and noise figures. The accuracy of circuit simulation is very crucial to meet these contraints and is strongly related to the accuracy of device models. Traditionally, the device models have focussed on the intrinsic behaviour of the transistor. Low frequency behaviour is modelled very accurately with MOS compact models such as BSIM [4], EKV [5] and MOS11 [6]. Operation at high frequency ($>$10GHz) of the device amplifies the extrinisic effects affecting the device performance. It is thus important to model both intrinsic and extrinsic effects [7]. Substrate resistance is an important extrinsic effect which needs to be modelled accurately for accurate device models.

At high frequencies, the signal at the drain couples to the source and the bulk terminals through the junction capacitance and the parastic substrate. This effects the small signal performance of

the device [8]. The output conductance Y_{22} shows a significant increase at high frequencies [9]. Y_{22} modeling error leads to a mismatch in impedance matching at the drain end degrading the performance of the circuit. The power loss in transistor is a function of the substrate resistance and is critical for amplifier design (ex. power amplifier design). These are some instances which illustrate the need for modelling substrate resistance to develop an accurate high frequency compact model.

In this report, the substrate network model is developed and a framework is designed to make the model scalable. Chapter 2 introduces and analyzes the various configurations possible to model the substrate coupling. Using 2-D and 3-D simulations, the best configuration is identified in Chapter 3. The framework to make the model scalable is presented in Chapter 4. In Chapter 5, analytical equations using Green's function are developed to enable calculation of the resistive components of the network and to develop scaling guidelines. Chapter 6 summarizes the work and outlines the future work.

Chapter 2

Substrate Networks

At low frequency, the influence of substrate resistance on the device performance is negligible and is ignored in compact modelling. However, at high frequency, the distributed resistance of the substrate effects the device performance. Ideally, a numerical solver for Poisson's equation in the substrate coupled with the intrinsic model will solve the problem, but given the computational overhead of such an approach, it is totally impractical. Using a distributed RC network is the next order simplification. The large number of nodes added by this approach discredits this approach too. To strike a balance between computational efficiency and accuracy, lumped RC network is used to model the substrate resistance. In this chapter, different configurations for lumped RC networks will be presented and analyzed.

2.1 Small-Signal Model at RF

The small signal model for the intrinsic device is a very well studied and accurate model. The AC small signal model at RF is built on top of it. For the AC model at RF, modelling of parasitics is very important. The model should be physics-based to ensure scalability and predictive capability without hurting the speed and performance of the model. The gate resistance [10] [11], the overlap capacitances and the substrate coupling network are required additions for high frequency modelling. Figure 2.1 shows the RF small signal model built around the low frequency intrinsic

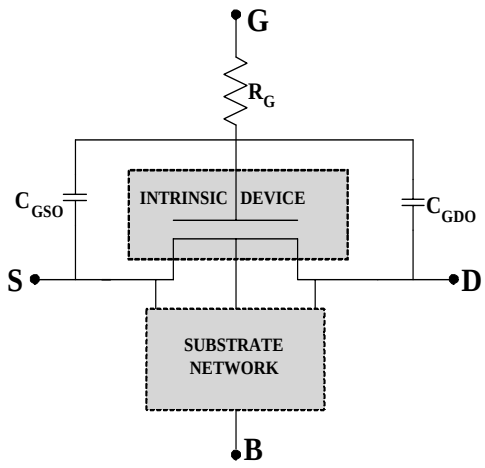

Figure 2.1: Small Signal Model at RF

model. A substrate network consists of the source and drain junction capacitances C_{js} and C_{jd}, through which the signals at drain and source couple to the substrate, and the resistor network in the substrate. It is the resistor network that models the resistive substrate which differs among the various substrate networks as will be seen shortly.

Y-parameters of a transistor will be used as a yardstick for the accuracy of any substrate network. Evaluating the Y-parameters analytically for the model in figure 2.1 is very cumbersome. When the gate voltage V_{gs} is smaller than the threshold voltage V_{th}, and the drain-source voltage V_{ds} is close to zero, most intrinsic components are negligble and the model in figure 2.1 reduces to a simple equivalent circuit as shown in figure 2.2. Hence, Y-parameters for all the substrate network configurations will be calculated for the off-state transistor to simplify the analysis.

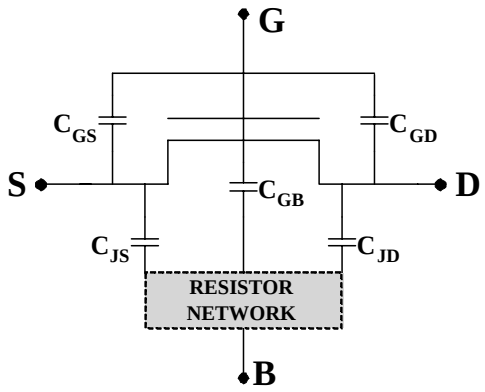

Figure 2.2: Off-state RF small signal model

2.2 Y-parameters and S-parameters

MOSFET is essentially a 4 terminal, 2-port device. For our purpose, bulk and source terminals are grounded. Gate and source terminals form the input port. The output port is between drain and source terminals. Y-parameters for the two-port network shown in figure 2.3 are defined as

$$Y_{ij} = \frac{I_i}{V_j} \mid_{V_k=0 \; for \; k \neq j} \tag{2.1}$$

which means that the admittance Y_{ij} is equal to the short-circuit current at port i when the port j is driven with unit voltage and the other port is short-circuited [12]. Y-parameters are useful at low frequencies because of the ease of measurement based on above definition. At high frequencies, Y-parameters are hard to measure due to need for broadband short circuits. As a result, S-parameters are measured at high frequencies, which are defined as

$$S_{ij} = \frac{V_i^-}{V_j^+} \mid_{V_k^+=0 \; for \; k \neq j} \tag{2.2}$$

which means that the scattering matrix element S_{ij} is the reflected wave amplitude V_i^- at port i when the incident wave V_j^+ on port j is unity and on all other ports is zero [12]. S-parameters are preferred at high frequency since they can be more easily measured.

In the theoretical analysis of substrate networks, 2-port Y-parameters will be used. For the experimental data, S-parameters of the MOSFETs will be measured and converted to Y-parameters using Open-Short de-embedding to remove the associated parastics [13].

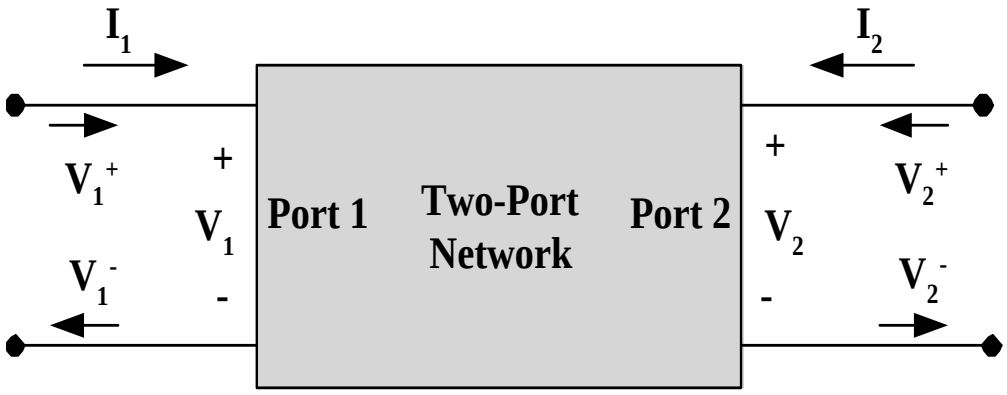

Figure 2.3: Two-port Network

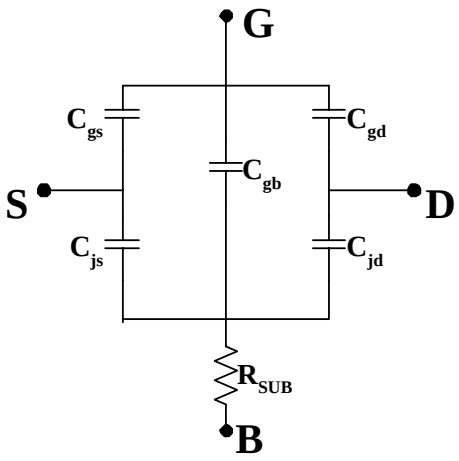

Figure 2.4: One Resistor Substrate Network

2.3 1-R Resistor Network

In the 1-R Resistor network, a single resistor is used to model the resistance between the device and the bulk terminal as shown in figure 2.4. The Y-parameters for the circuit are calculated in Appendix A. The low frequency approximations to the Y-parameters are simple and can be used for extraction as shown below. The imaginary parts of low frequency Y-parameters are :

$$Im[Y_{11}] = \omega(C_{gd} + C_{gs} + C_{gb}) \quad (2.3)$$

$$Im[Y_{12}] = -\omega C_{gd} \quad (2.4)$$

$$Im[Y_{21}] = -\omega C_{gd} \quad (2.5)$$

$$Im[Y_{22}] = \omega(C_{gd} + C_{jd}) \quad (2.6)$$

and the corresponding real parts are :

$$Re[Y_{11}] = \omega^2 R_{SUB} C_{gb}^2 \quad (2.7)$$

$$Re[Y_{12}] = \omega^2 R_{SUB} C_{jd} C_{gb} \quad (2.8)$$

$$Re[Y_{21}] = \omega^2 R_{SUB} C_{gb} C_{jd} \quad (2.9)$$

$$Re[Y_{22}] = \omega^2 R_{SUB} C_{jd}^2 \quad (2.10)$$

The network component values can be extracted from the low frequency simulation data or

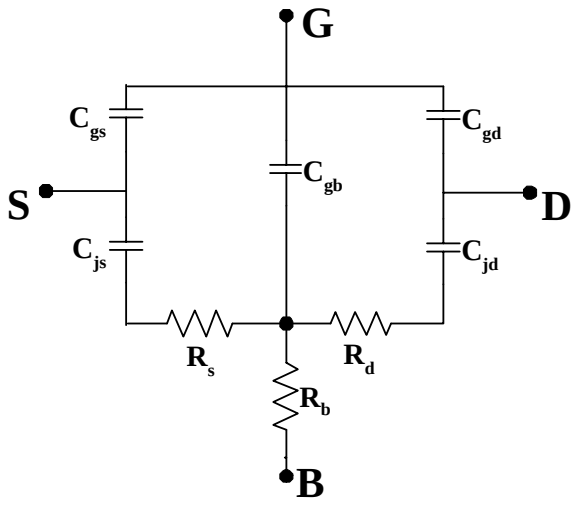

Figure 2.5: Three Resistor Substrate Network

experimental Y-parameter data using above equations. C_{gd} is obtained from $Im[Y_{12}]$. Assuming a symmetric device (C_{gs} = C_{gd}), C_{gb} is then obtained from $Im[Y_{11}]$. Finally, the junction capacitances C_{jd} = C_{js} are extracted from $Im[Y_{22}]$.

The resistor R_{SUB} can be extracted from any one of the four real Y-parameters. To perform an unbiased comparison among all networks, we chose to extract R_{SUB} from $Re[Y_{11}]$. The model accuracy will be tested by comparing the model and simulation data at high frequency.

2.4 3-R Resistor Network

The 3-R network builds upon the 1-R network by adding resistive losses between source-drain signal coupling. R_s and R_d are added to 1-R network to give the new configuration as shown in figure 2.5. The trade-off involved with this network is the addition of two new nodes for each device which leads to model speed reduction. The Y-parameters and their low frequency approximations for this circuit are calculated in Appendix B. The imaginary parts of Y-parameters are identical to the 1-R network equations 2.3 - 2.6 and hence not repeated. The real parts are :

$$Re[Y_{11}] = \omega^2 R_b C_{gb}^2 \tag{2.11}$$

$$Re[Y_{12}] = \omega^2 R_b C_{jd} C_{gb} \tag{2.12}$$

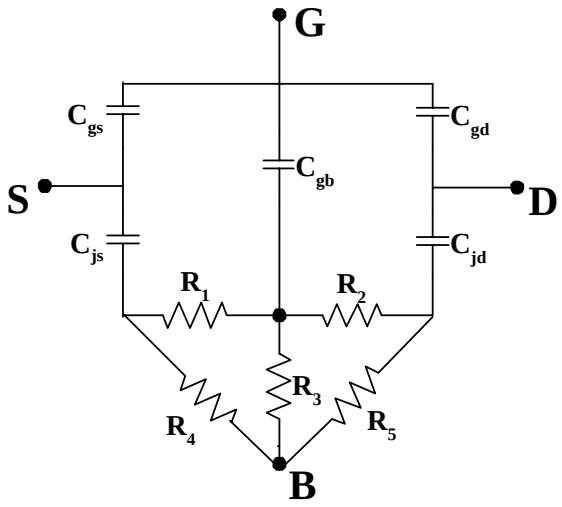

Figure 2.6: Five Resistor Substrate Network

$$Re[Y_{21}] = \omega^2 R_b C_{gb} C_{jd} \tag{2.13}$$

$$Re[Y_{22}] = \omega^2 (R_b + R_d) C_{gb}^2 \tag{2.14}$$

The network components are extracted using the above low frequency approximations to the Y-parameters. The capacitance extraction follows the same algorithm as that of 1-R network since the imaginary Y-parameters are identical. To keep consistency among comparisons, R_b is extracted from $Re[Y_{11}]$. The remaining resitance value R_s = R_d is extracted from $Re[Y_{22}]$. Note that though the equations are derived for an asymmetric device, the extraction procedure is developed for a symmetric device. Model checking is performed against high-frequency Y-parameter data.

2.5 5-R Resistor Network

The 5-R network (figure 2.6) improves upon the 3-R network by presenting resistive paths from source to bulk and drain to bulk. Compared with the 1-R network, this network model also requires two extra nodes and hence exhibits model speed reduction. However, its speed will be comparable with the 3-R network. The network is very complex for analysis as can be seen in Appendix C. At low frequecies, the complex expressions simplify to a very large extent. The imaginary parts of the low frequency Y-parameters are again identical to those of 1-R network resutling in identical

extraction procedure for the capacitances. The real parts of Y-parameters are listed below :

$$Re[Y_{11}] = \omega^2 C_{gb}^2 \overbrace{R_3||(R_1+R_4)||(R_2+R_5)} = \omega^2 C_{gb}^2 R11 \quad (2.15)$$

$$Re[Y_{12}] = \omega^2 C_{jd} C_{gb} \overbrace{\frac{R_5}{R_5+R_2} R11} = \omega^2 C_{jd} C_{gb} R12 \quad (2.16)$$

$$Re[Y_{12}] = \omega^2 C_{gb} C_{jd} \frac{R_5}{R_5+R_2} R11 \quad (2.17)$$

$$Re[Y_{22}] = \omega^2 C_{jd}^2 \overbrace{R12(1+\frac{R_2}{R_3}+\frac{R_2}{R_1+R_4})} = \omega^2 C_{jd}^2 R22 \quad (2.18)$$

For a symmetrical device, there are three distinct resistances R_1 = R_2, R_3 and R_4 = R_5. The values of these three resistances are extracted by solving equations 2.15, 2.16 and 2.18 simultaneously, which turns out to be a fairly simple excercise.

2.6 Verification

All the above equations have been verified using the circuit simulator SPICE. The equivalent circuits for each case were constructed in SPICE with different component values and the low frequency Y-parameters were observed. The SPICE data agreed exactly with the low frequency approximations in all the cases, validating the above derivations and the extraction procedures.

Chapter 3

Substrate Network Identification

In the previous chapter, different possible substrate network configurations were analyzed. The 1-R and the 3-R networks and their variants have been studied earlier by various researchers [14] [15] [16] [17] [18] [19] and shown to agree with data, but the study was mostly limited to $Re[Y_{22}]$. In this work, focus is on all Y-parameters. The simulation studies performed to identify the accurate substrate network are described in this chapter.

3.1 2-D Simulations

2-D device simulations were performed using the device simulator MEDICI. An NMOS device with channel length 0.18 μm and an oxide thickness t_{ox} of 20 $\overset{o}{A}$ was simulated. In order to consider a general case, gaussian doping profile was used in the substrate. Figure 3.1 shows the doping profile in the substrate normal to the oxide-silicon interface. Y-parameters of the device were measured at a gate bias $V_{gs} - V_{th} \approx -0.4V$ so that the device is in the off-state and no drain bias V_{ds} was applied.

Y-parameters measured at a low frequency of 1kHz were used to extract the component values of all the three substrate networks. Using equations 2.3 to 2.6, the capacitances C_{gs}, C_{js} and C_{gb} were extracted. Note that the simulated device is symmetric since the extraction procedure

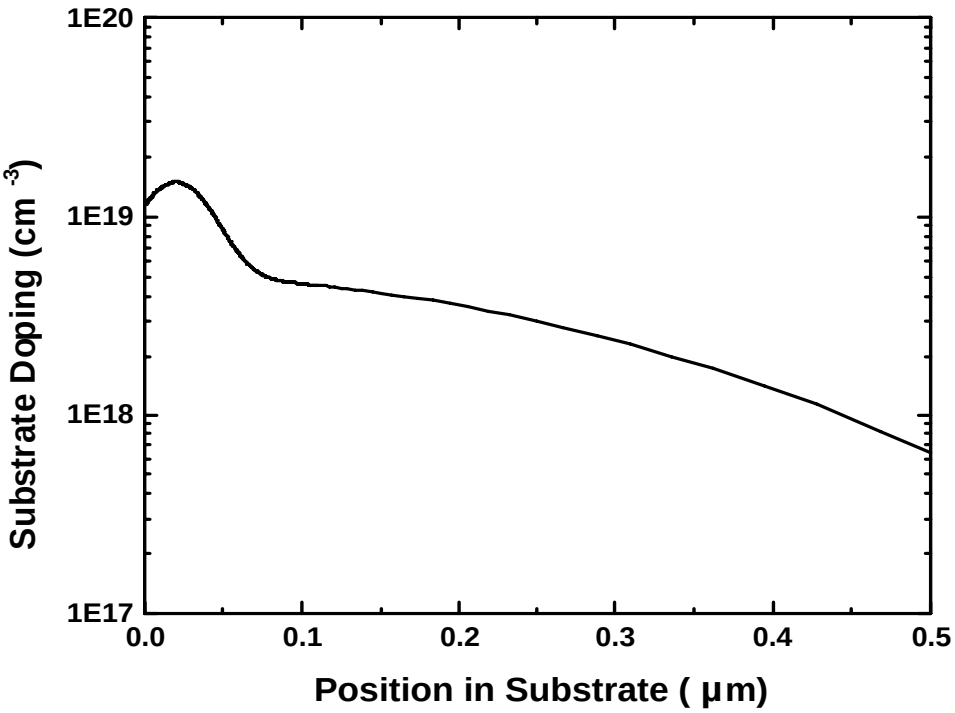

Figure 3.1: Doping Profile in Substrate

developed in previous chapter assumes symmetric devices. The 1-R newtork resistor is extracted first. Using equation 2.7, R_{SUB} was found to be 811Ω. For the 3-R network, from equations 2.11 and 2.14, the resistor values were extracted to be R_b = 811Ω and R_d = 42.4Ω. For the 5-R network, the values of resistors obtained using equations 2.15, 2.16 and 2.18 are R_1 = 81.46Ω, R_3 = 1520Ω and R_5 = 3395Ω.

Using these extracted values, Y-parameters were calculated at higher frequencies and compared with the simulation data. For the imaginary Y-parameters, all three network models gave good prediction and hence are not shown here. The 5-R network showed the best agreement with the imaginary part among all three networks. Figures 3.2, 3.3 and 3.4 show the real Y-parameter simulation data and the prediction data from all the three substrate networks. From figure 3.2, all the three substrate networks show good agreement with $Re[Y_{11}]$. For $Re[Y_{22}]$, there is a mismatch of about 10% using the 1-R resistor network (figure 3.3). It is important to note that one can fit $Re[Y_{22}]$ using the 1-R network at the expense of $Re[Y_{11}]$ by using equation 2.10 to extract R_{SUB}. For $Re[Y_{12}]$, both the 1-R and 3-R networks show a mismatch of 5-10% as seen in figure 3.4.

Based on the above observations, the 1-R network and 3-R network are ruled out in circuit ap-

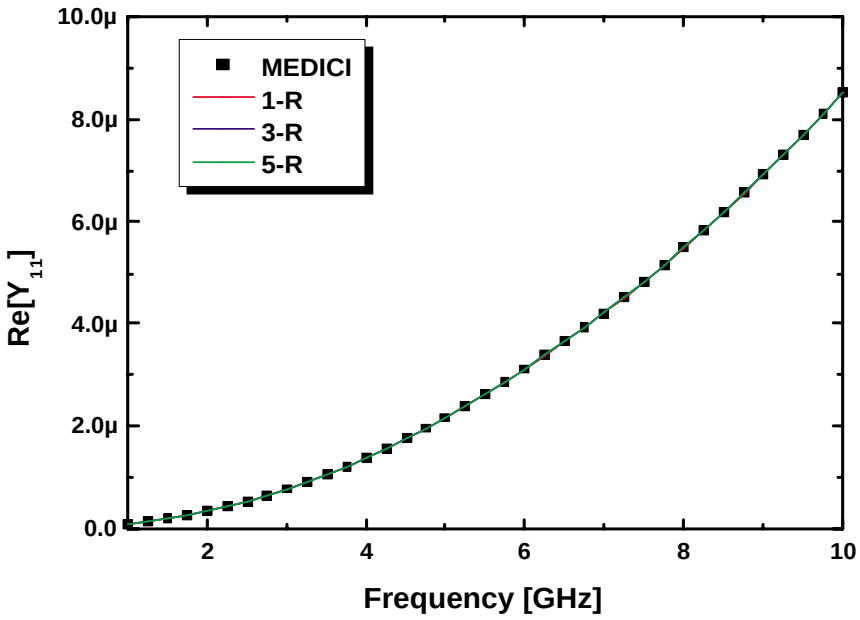

Figure 3.2: Simulated and Predicted Re[Y_{11}]

plications requiring accuracy higher than 10% on Y-parameters. 5-R resistor network is evidently the most superior network model since it predicts all the Y-parameters well. The accurate substrate network is thus identified to be the 5-R resistor network. It is useful to note that in applications that not are highly sensitive to substrate resistance, the 1-R network can be put into use because it is more computationally efficient with two fewer nodes than the other two networks.

In order to validate above results and check the physical nature of resistances, more simulations were performed. In one particularly interesting study, the surface doping was fixed at 5E18 cm^{-3} while the substrate doping was varied from 1E19 cm^{-3}, 5E18 cm^{-3} and 1E18 cm^{-3}. In all the cases, 5-R network model showed the best agreement with simulation data. Figure 3.5 shows the deviation between simulation data and model prediction for all Y-parameters for the case of 1E19 cm^{-3} substrate doping. The 5-R substrate network predicts all Y-parameters within 1% accuracy as seen from figure 3.5. Table 3.1 shows the extracted resistance values for the 5-R network model for the above simulation cases. As the substrate doping increases, the resistances increase indicating their physical nature.

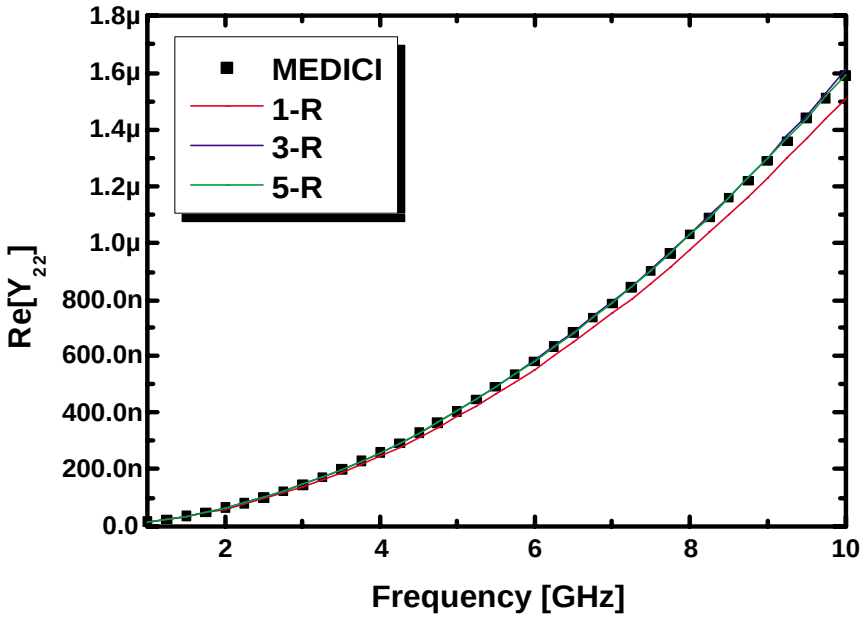

Figure 3.3: Simulated and Predicted Re[Y_{22}]

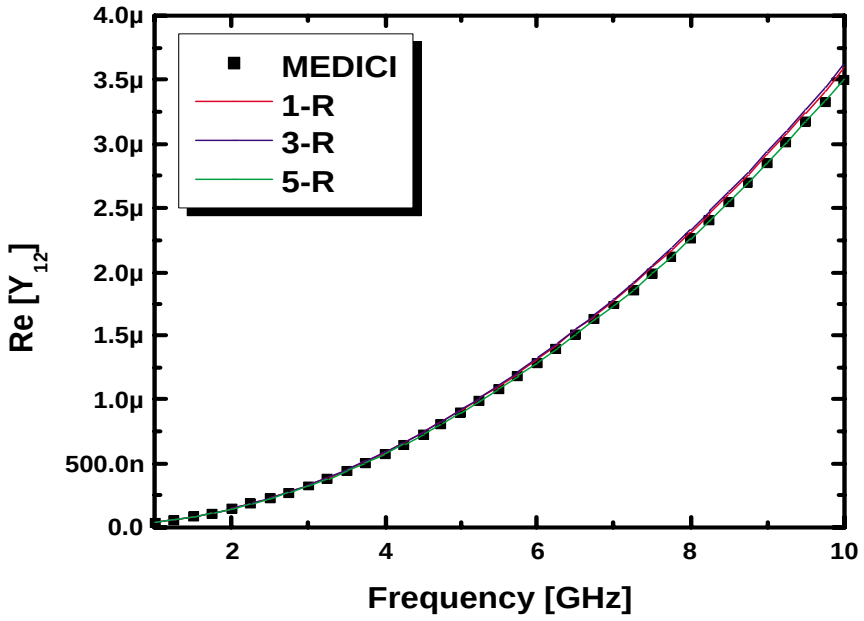

Figure 3.4: Simulated and Predicted Re[Y_{12}]

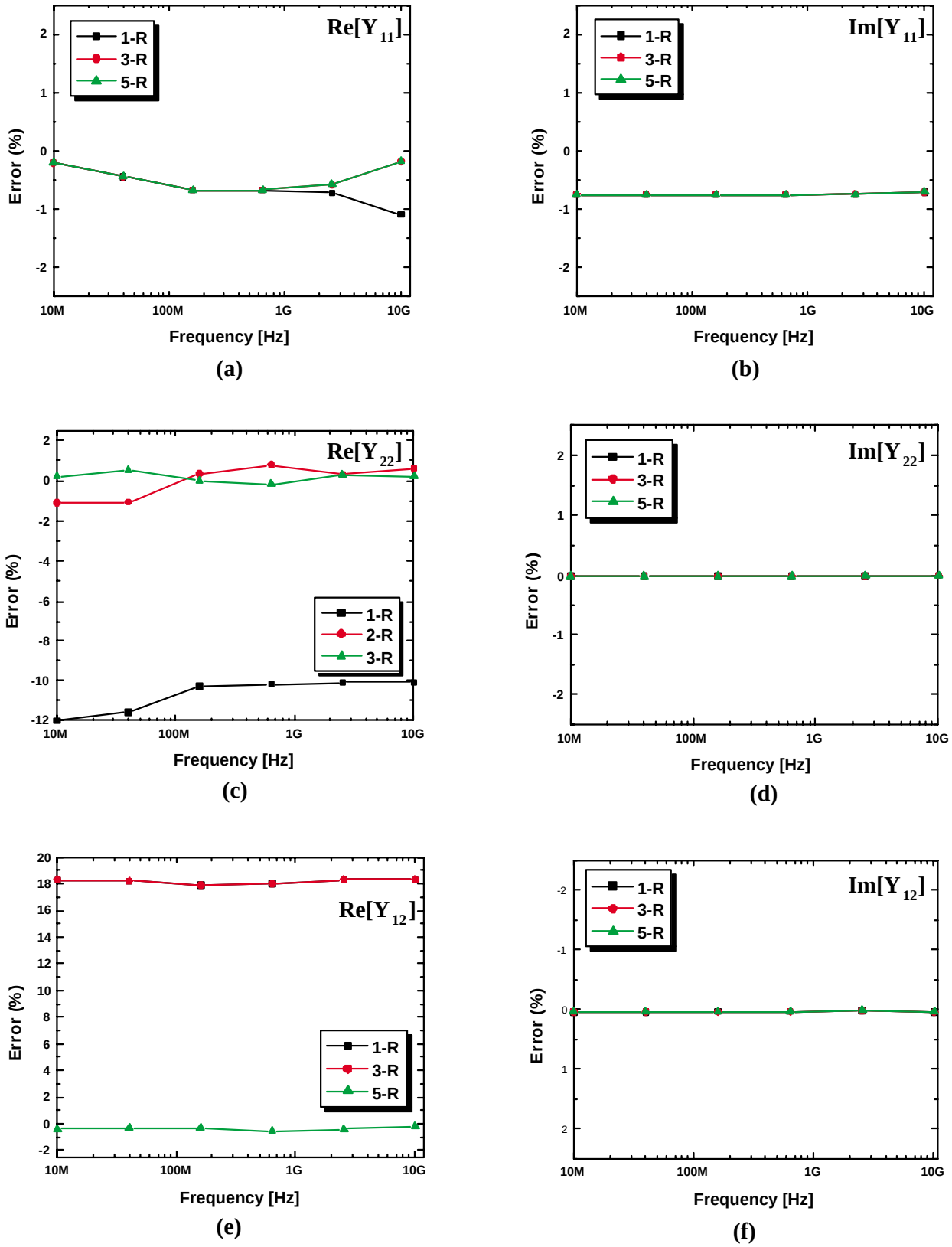

Figure 3.5: Error between the simulated and predicted data for all the real and imaginary *Y*-parameters for NMOS with 5E18 cm^{-3} surface doping and 1E19 cm^{-3} substrate doping.

Substrate Doping (cm^{-3})	R_1 (Ω)	R_3 (Ω)	R_5 (Ω)
1E19	109	668	587
5E18	127	918	1034
1E18	160	3138	2540

Table 3.1: Variation of resistances of 5-R network with substrate resistance

3.2 3-D Simulations

3-D simulations were performed using the 3-D device simulator ISETCAD. The substrate contact arrangements come in essentially two different flavors. In the vertical contact arrangement, the substrate contacts are placed parallel to the width of the device. In the horizontal contact arrangement, the contacts are placed perpendicular to the width of the device. Simulations were performed with both kind of arrangements. A combination of these two arrangements, all-around contact arrangement, is also used frequently to further reduce the substrate resistance by providing more contacts. In this arrangement the device is surrounded by substrate contacts on all sides.

Figure 3.6 shows the simulated vertical contact arrangement in which the substrate contacts are placed 0.25μm apart from the device edges. The 5-R substrate network model shows excellent agreement with the simulations (figure 3.7). Only the real part of Y-parameter data is shown. A similiar excercise was performed with the horizontal contact arrangement, Fig. 3.8, with the substrate contacts again placed 0.25μm apart from the device edges, and the results are shown in figure 3.9.

Thus, 5-R substrate network is the substrate network of choice. The 5-R network has been shown to be capable of modelling the substrate for both kind of substrate contact layouts. An attempt will be made to develop a scalable model for the 5-R network in the future chapters.

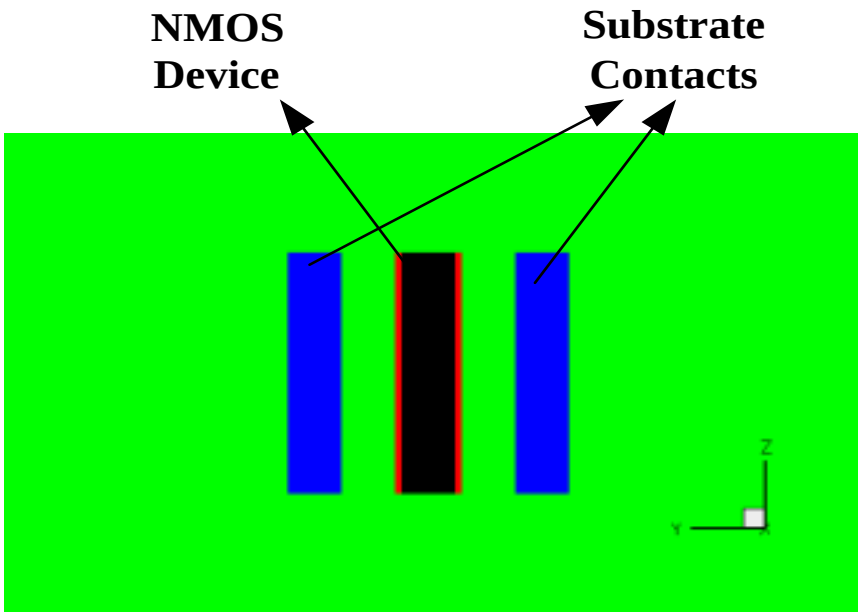

Figure 3.6: Vertical Substrate Contact Structure

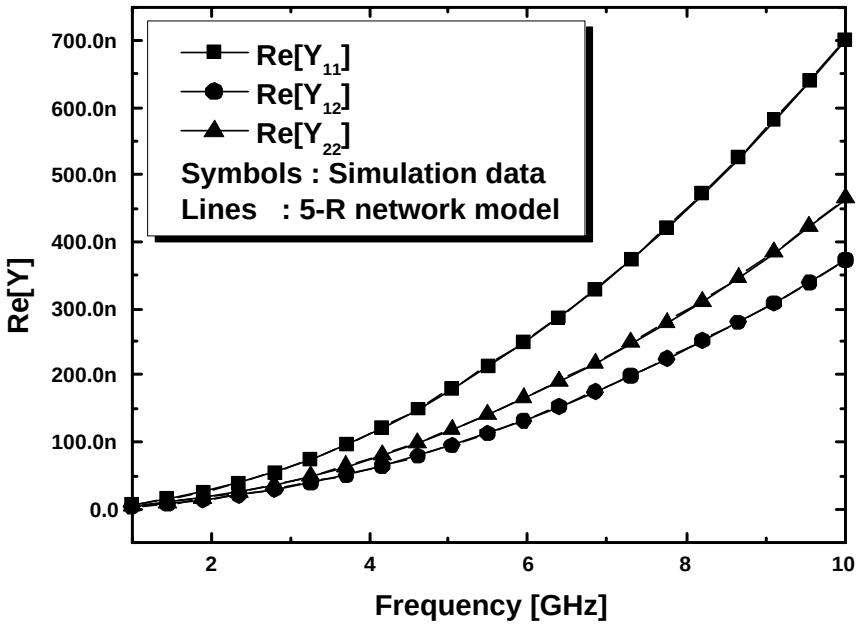

Figure 3.7: Simulated and Predicted Re[Y]

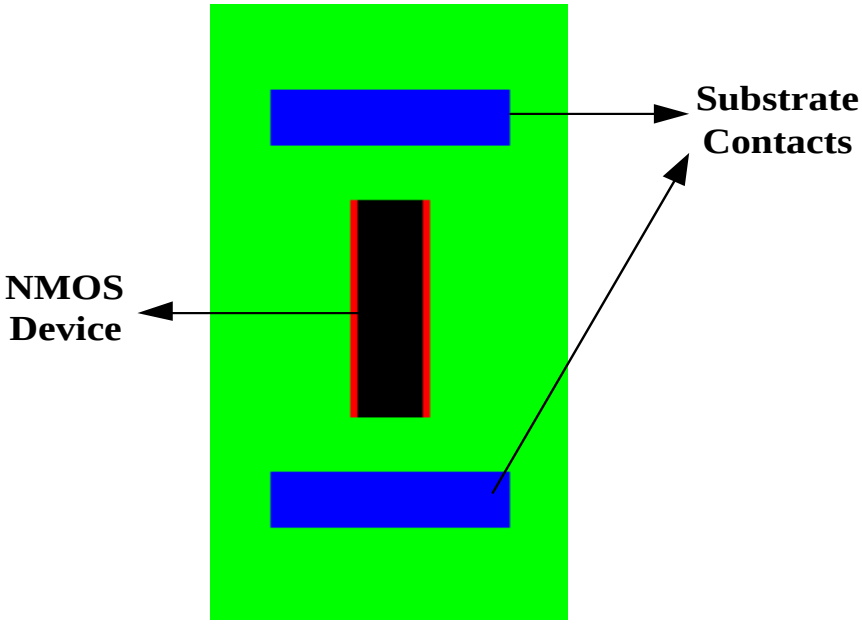

Figure 3.8: Horizontal Substrate Contact Structure

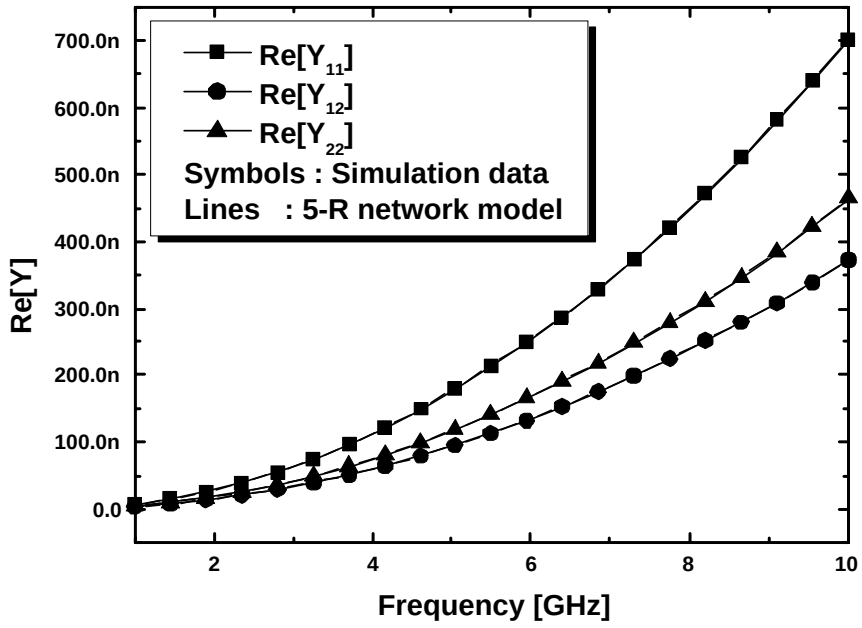

Figure 3.9: Simulated and Predicted Re[Y]

Chapter 4

Scalable Model

In the previous chapter, the 5-R substrate network was identified to be the accurate network. It is highly advantageous to make the substrate network model scalable in order to avoid individual resistance extraction procedure for all transistors. In this chapter, a scalable model will be proposed with the list of scaling parameters. From now on, the term substrate network will imply the 5-R network unless otherwise specified.

4.1 Multi-Finger Transistor

Till now, the 5-R network has been discussed from a single finger transistor point of view. The equivalent 5-R network for a multi-finger transistor with *NF* fingers, N_s sources and N_d drains will be developed in this section. For a multi-finger transistor, a substrate network exists for each finger. Figure 4.1 shows the equivalent substrate network for a *NF* = 3 multi-finger transistor with one substrate contact. For the purpose of compact modelling, it is reasonable to assume that all the imaginary source nodes S_i, the imaginary drain nodes D_i and the imaginary bulk nodes B_i form a set of equipotential nodes within themselves. As a result, all the resistors ${R_i}^j$ for a fixed *i* are parallel to each other. The same holds for the capacitances since the terminals source, drain and gate are obviously at the same potential. There are *NF* number of ${R_1}^j$, ${R_2}^j$ and ${R_3}^j$ resistors, N_s number of ${R_4}^j$ resistors and N_d number of ${R_5}^j$ resistors. Using these facts, all the 5-R networks

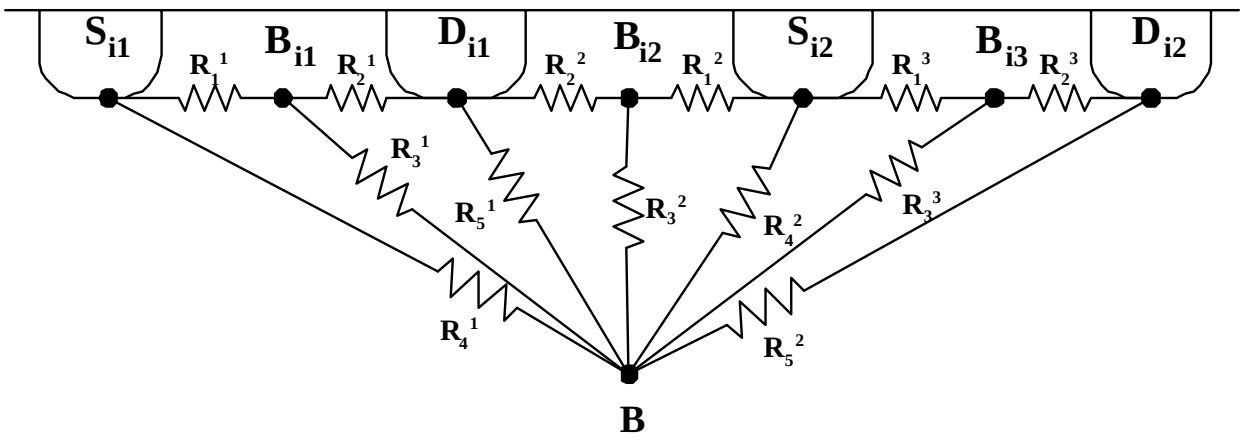

Figure 4.1: Equivalent Substrate Network for *NF* = 3 device

can be combined to form a single 5-R network whose elements will be given by

$$\frac{1}{R_i^{total}} = \sum_{j=1}^{NF} \frac{1}{R_i^j} \qquad i = 1, 2, 3 \tag{4.1}$$

$$\frac{1}{R_4^{total}} = \sum_{j=1}^{N_s} \frac{1}{R_4^j} \tag{4.2}$$

$$\frac{1}{R_5^{total}} = \sum_{j=1}^{N_d} \frac{1}{R_5^j} \tag{4.3}$$

Thus, one can reduce the substrate network for a multi-finger device to the form of single-finger substrate network easily. These equations will provide valuable insight while dealing with the scalability of the model with respect to number of fingers.

4.2 Scalable model

It is desirable to make the substrate network scalable. One needs to identify the physical parameters with respect to which scaling is important. In this work, scaling of the model is observed with respect to the channel length *L*, the channel width *W* and the number of fingers *NF*. To get an insight into the scaling of the individual resistors of the substrate network, an analogous distributed resistance case is considered in which the imaginary nodes of the 5-R network are replaced by imaginary surface contacts. As shown in figure 4.2, the resistors of the network are equivalent to the resistors between the imaginary surface contacts S_i, B_i, D_i and the real bulk contact *B*. The

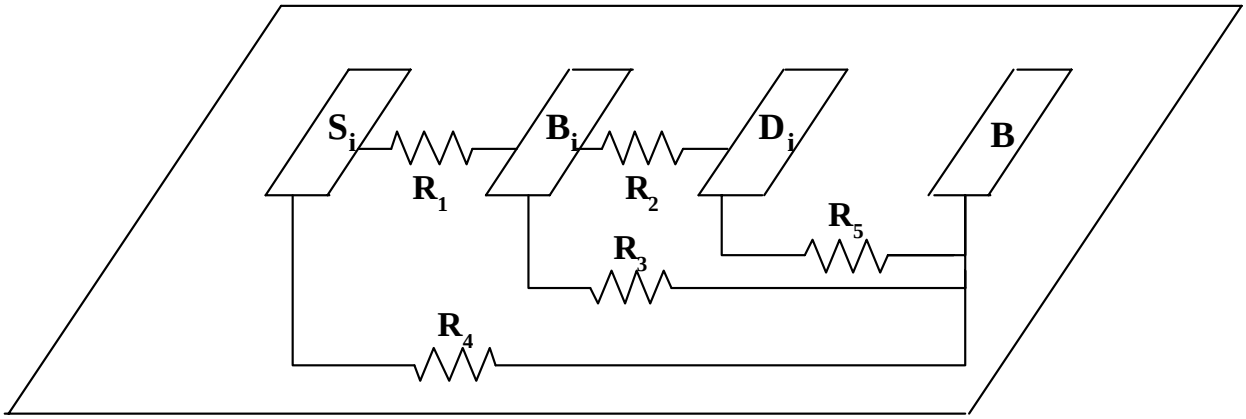

Figure 4.2: Equivalent Imaginary Surface Contacts Representation

values of the resistors can be calculated analytically using Green's function as will be shown in the next chapter. A simple scalable model can be now developed with this equivalent picture in mind. All the resistors will scale as

$$R_i = R_{i0}\ L^{\alpha}\ W^{\beta}\ NF^{\gamma} \tag{4.4}$$

where α, β and γ are scaling parameters. In a general contact arrangement, substrate contacts can be vertical and horizontal. There is no reason for the scaling parameters of resistances to the vertical contact and resistances to the horizontal contact to be identical. Each resistor of the network can be taken as a parallel combination of the resistor to the vertical contact R_{VERT} and the resistor to the horizontal contact R_{HORI}. Hence, a general scalable model can be developed as

$$\begin{aligned} R_i &= R_{i_{HORI}} \parallel R_{i_{VERT}} \\ R_{i_{HORI}} &= R_{i0_x}\ L^{\alpha_x}\ W^{\beta_x}\ NF^{\gamma_x} \\ R_{i_{VERT}} &= R_{i0_y}\ L^{\alpha_y}\ W^{\beta_y}\ NF^{\gamma_y} \end{aligned} \tag{4.5}$$

The general model will consist of $5 \times 2 \times 4 = 40$ parameters. This is a large number of parameters for any compact model and should be reduced if possible.

	HORIZONTAL CONTACT				VERTICAL CONTACT			
	$\mathbf{R}_{0x}$	α_x	β_x	γ_x	$\mathbf{R}_{0y}$	α_y	β_y	γ_y
$\mathbf{R}_1$	1/1	2/2	3/3	4/4	NR	NR	NR	NR
$\mathbf{R}_2$	5/1	6/2	7/3	8/4	NR	NR	NR	NR
$\mathbf{R}_3$	9/5	10/6	11/7	12/8	13/9	14/10	15/11	16/12
$\mathbf{R}_4$	17/13	18/14	19/15	20/16	21/17	22/18	23/19	24/<u>20</u>
$\mathbf{R}_5$	25/13	18/14	19/15	20/16	<u>26</u>/17	22/18	23/19	24/20

Table 4.1: Parameter Reduction Table

4.3 Parameter Reduction

The scalable model developed in the previous section has 40 parameters. This model does not try to take into account any symmetries in the structure. By taking the symmetries into account, the parameter set can be reduced to 26 parameters for an assymetric device and 20 parameters for symmetric device as tabulated in Table 4.1. If the substrate contacts are restricted only to one kind of arrangement : vertical or horizontal, the number of parameters reduce further to 17 for an assymetric device and 12 for a symmetric device. This reduction can be easily deduced from the table. The table shows the parameters needed for a scalable 5-R substrate network. The numbers in the table keep a track of the count of parameters. The first number of each cell represents the count for asymmetric device parameter set and the second number is the count for symmetric device parameter set. The rationale behind the table is explained below. Approximate values of the parameters are also presented wherever possible.

The resistors R_1 and R_2 are the resistances between the nodes $\{S_i, B_i\}$ and between $\{D_i, B_i\}$ respectively. Hence, they need not differentiate between the vertical and horizontal contact arrangements. Separate parameters are not needed for the two arrangements for R_1 and R_2 as indicated by *NR* (Not Required) in the table. This reduces the number of parameters by 8. Further, if the device is symmetric, scaling parameters will be identical for both R_1 and R_2 and the number of parameters further decrease by 4 as shown in the table. In a multi-finger device, since all ${R_1}^j$ and ${R_2}^j$ are identical, using equation 4.1, one can evaluate $\gamma \approx$ -1. For a device with large width and small channel length, where the fringing between two imaginary contacts can be neglected, $\alpha \approx 1$ and $\beta \approx$ -1 for the resistors R_1 and R_2.

The resistors R_3, R_4 and R_5 terminate on the substrate contacts and hence need seperate scaling parameters for the horizontal and vertical contacts case. R_4 and R_5 are expected to have same scaling laws by symmetery. This further reduces the number of parameters by 6 since the scaling parameters α, β and γ in both *x* and *y* direction are identical. However, for a symmetric device, all the 8 parameters of R_4 and R_5 are identical. For a wide device, one can assume $\beta_y \approx -1$ for all resistors. Scaling with *NF* is not trivial for these 3 resistors, since the resistors R_i^j for *i = 3, 4, 5* are different for different *j* and equations 4.1, 4.2 and 4.3 need to be used.

By using simple symmetries, huge gain is achieved in reducing the number of parameters. To develop further guidelines for calculating scaling parameters, the resistors need to be evalauated analytically for different device dimensions. This is done through the use of Green's function which is the subject of the next chapter.

Chapter 5

Green's Function

It is neccessary to be able to estimate the model component values to make the model scalable. In this respect, one needs to develop analytical equations to calculate the resisor values of the substrate network (figure 2.6). The substrate doping profile in modern devices is highly complex. To keep the analysis simple and accurate, we can model the substrate as consisting of single layer with an effective uniform doping value. Adding a second layer can help in using a step profile in substrate or in simulating the true boundary condition at the bottom of well using a highly resistive bottom layer as explained later. Imaginary contacts replace the nodes S_i, D_i and B_i. The highly complex problem of distributed resistance of the substrate is thus reduced to evaluating the resistors between surface contacts in a two-layered substrate.

Two main approaches to this problem are the numerical technique and an integral-equation method. The resistances are extracted in both cases by solving the differential equations of the substrate. Within the numerical technique, Laplace equation with appropriate boundary conditions is solved in the susbtrate by approximating the differential equations of system using difference equations [20]. The numerical technique is very time consuming and will not generate any analytical equations. Hence, the integral-equation method based on Green's function is used in this work.

The Green's function for multi-layer substrate is outlined in [21] [22] for capacitance calculation. The equivalent Green's function for resistance calculation for a 2-layer substrate is derived

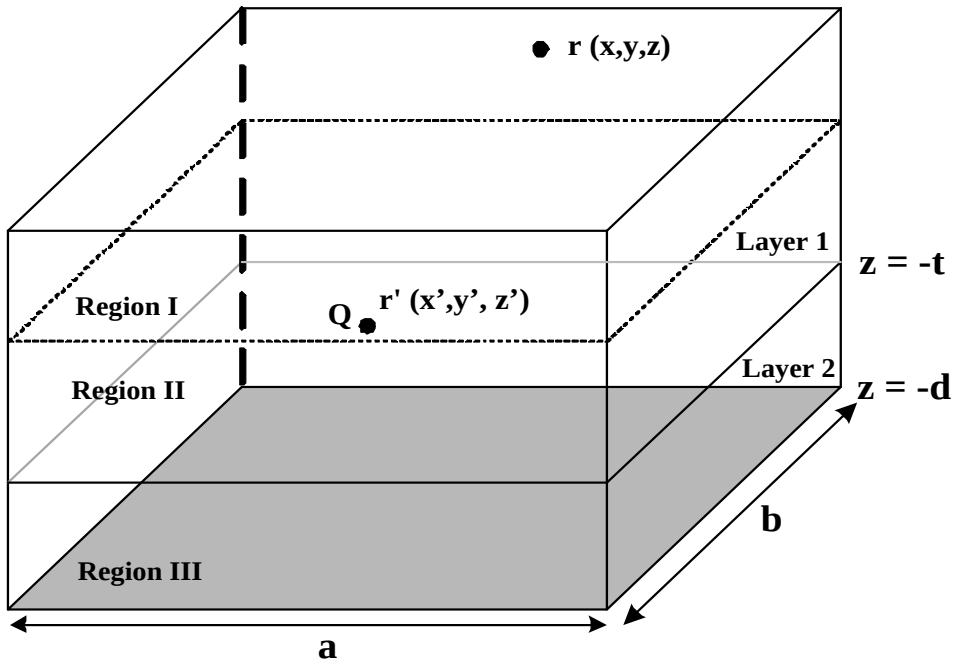

Figure 5.1: 2 Layered Substrate Model

in this chapter. The assumptions made during the derivation of Green's function are worth noting. There is no inductive reactance between the contacts for frequencies of interest. Boundary conditions are limited to Neumann (zero normal E-field) and Dirichlet (zero potential) and any radiation field is ignored. The conductivity of substrate is assumed to be constant and independent of electric field. The Green's function is evaluated first and then applied to extract substrate resistance.

5.1 2-layer Green's Function

Green's function $G(r, r^{'})$ is defined as the potential at location r in the medium due to a point charge **Q** located at $r^{'}$ as shown in figure 5.1. Using the Poisson's equation, $G(r, r^{'})$ satisfies

$$\bigtriangledown^2 G(r, r^{'}) = -\frac{\rho(r - r^{'})}{\epsilon} \tag{5.1}$$

Expressing $G(r, r^{'})$ in seperable of variables form as

$$G(r, r^{'}) = X(x, x^{'})Y(y, y^{'})Z^{'}(z, z^{'}) \tag{5.2}$$

the Poisson's equation 5.1 can be transformed into

$$YZ^{'}\frac{d^2X}{dx^2} + Z^{'}X\frac{d^2Y}{dy^2} + XY\frac{d^2Z^{'}}{dz^2} = -\frac{\delta(x-x^{'})\delta(y-y^{'})\delta(z-z^{'})}{\epsilon} \tag{5.3}$$

Since the normal E-field is zero on the sidewalls, assume $X = \cos(\frac{m_1\pi x}{a}); Y = \cos(\frac{n_1\pi y}{b})$ where m_1, $n_1 \in [0,\infty)$. Substituting it in equation 5.3,

$$\sum_{m_1=0}^{\infty}\sum_{n_1=0}^{\infty}\cos\Big(\frac{m_1\pi x}{a}\Big)\cos\Big(\frac{n_1\pi y}{b}\Big)\Big\{\frac{d^2Z^{'}}{dz^2} - \Big(\Big(\frac{m_1\pi}{a}\Big)^2 + \Big(\frac{n_1\pi}{b}\Big)^2\Big)Z^{'}\Big\} = -\frac{\delta(x-x^{'})\delta(y-y^{'})\delta(z-z^{'})}{\epsilon} \tag{5.4}$$

Multiplying equation 5.4 by $\cos(\frac{m\pi x}{a})\cos(\frac{n\pi y}{b})$ and integrating over the variables *x* (0 $\longrightarrow$ a) and *y* (0 $\longrightarrow$ b), we get

$$\frac{ab}{4}\Big\{\frac{d^2Z^{'}}{dz^2} - \Big(\Big(\frac{m_1\pi}{a}\Big)^2 + \Big(\frac{n_1\pi}{b}\Big)^2\Big)Z^{'}\Big\} = -\frac{\delta(z-z^{'})}{\epsilon}\cos\Big(\frac{m\pi x^{'}}{a}\Big)\cos\Big(\frac{n\pi y^{'}}{b}\Big) \tag{5.5}$$

Substituting $Z^{'} = Z\cos(\frac{m\pi x^{'}}{a})\cos(\frac{n\pi y^{'}}{b})$ in equation 5.5, we get

$$\frac{ab}{4}\Big\{\frac{d^2Z^{'}}{dz^2} - \gamma_{mn}^2 Z\Big\} = -\frac{\delta(z-z^{'})}{\epsilon} \tag{5.6}$$

where $\gamma_{mn} = \sqrt{(\frac{m\pi}{a})^2 + (\frac{n\pi}{b})^2}$. For the case $z \neq z^{'}$, the differential equation has the general solution

$$Z = \alpha\cosh(\gamma_{mn}z) + \beta\sinh(\gamma_{mn}z) \tag{5.7}$$

The whole substrate is divided into 3 regions as shown in figure 5.1. In region I, the normal E-field at surface is zero. In region III, the potential at the bottom surface is zero. Using these boundary condtions, the general solutions for $Z(z,z^{'})$ are

$$\begin{aligned} Z(z,z^{'}) &= \alpha_1\cosh(\gamma_{mn}z) && z \in I \\ &= \alpha_2\cosh(\gamma_{mn}z) + \beta_2\sinh(\gamma_{mn}z) && z \in II \\ &= \alpha_3\sinh(\gamma_{mn}(d+z)) && z \in III \end{aligned} \tag{5.8}$$

To solve for the four unknowns in equation 5.8, boundary conditions at interface between the two interfaces are used. Since the potential is continuous across the interface,

$$Z_I\Big|_{z=z^{'}} = Z_{II}\Big|_{z=z^{'}} \tag{5.9}$$

$$Z_{II}\Big|_{z=-t} = Z_{III}\Big|_{z=-t} \tag{5.10}$$

Continuity of normal component of current density at the interface between the two layers with different conductivity requires

$$\sigma_1 \frac{dZ_{II}}{dz}\Big|_{z=-t} = \sigma_2 \frac{dZ_{III}}{dz}\Big|_{z=-t} \tag{5.11}$$

The last boundary condition is obtained by integrating the differential equation 5.6

$$\frac{dZ_I}{dz}\Big|_{z=z'} - \frac{dZ_{II}}{dz}\Big|_{z=z'} = -\frac{4}{ab\epsilon} \tag{5.12}$$

For the structure under consideration, which has surface contacts, the relevant Green's function is obtained from Z_I. The variable α_1 is obtained by solving equations 5.8 to 5.12. Since surface contacts are of interest, set $z = 0, z^{'} = 0$ in expression for $Z_I(z, z^{'})$ to obtain $Z^{'}(0,0)$. Using $Z^{'}(0,0)$ in equation 5.2, the Green's function is

$$G = \sum_{m_1=1}^{\infty}\sum_{n_1=1}^{\infty}\left\{\frac{4}{ab\epsilon\gamma_{mn}}\frac{\cosh(\gamma_{mn}t)\sinh(\gamma_{mn}(d-t)) + \frac{\sigma_2}{\sigma_1}\cosh(\gamma_{mn}(d-t))\sinh(\gamma_{mn}t)}{\sinh(\gamma_{mn}(d-t))\sinh(\gamma_{mn}t) + \frac{\sigma_2}{\sigma_1}\cosh(\gamma_{mn}(d-t))\cosh(\gamma_{mn}t)}\right\} \tag{5.13}$$
$$\times \cos\left(\frac{m\pi x^{'}}{a}\right)\cos\left(\frac{m\pi x}{a}\right)\cos\left(\frac{n\pi y^{'}}{b}\right)\cos\left(\frac{n\pi y}{b}\right)$$

Note that the summations start from $m = 1$ and $n = 1$. For the indices $m \neq 0, n = 0$ and $n \neq 0, m = 0$, the equation 5.5 changes and it has only one appropriate cosine term and 4 is replaced by 2. When the analysis is repeated from equation 5.5 to 5.13, it is trivial to see that the resulting Green's function has only one summation and 4 is repalced by 2. For the case of $m = 0, n = 0$, in the equation 5.5, 4 is replaced by 1 and the general solution for differential equation 5.6 becomes

$$Z = \alpha + \beta z \tag{5.14}$$

By applying the boundary conditions to equation 5.14 in the three regions of the substrate and solving in a similiar fashion to the case $m \neq 0, n \neq 0$, we get

$$G = \frac{d-t}{\frac{\sigma_2}{\sigma_1}ab\epsilon} + \frac{t}{ab\epsilon} \tag{5.15}$$

The final Green's function for the substrate is obtained by adding together the Green's functions for all the four cases : $m \neq 0, n \neq 0$; $m \neq 0, n = 0$; $m = 0, n \neq 0$; and $m = 0, n = 0$.

5.2 Substrate Resistance Extraction

Using the Green's function from previous section, the substrate resistances will be extracted. Suppose a charge *Q* is placed on a contact. The current flowing from the positively charged conductor is equal to [23]

$$I = \oint_{surface} \vec{J} \cdot d\vec{a} \tag{5.16}$$

where the surface intergal is taken over a surface that encloses the positively charged contact. The expression of the current can be rewritten in terms of the electric field as

$$I = \sigma \oint_{surface} \vec{E} \cdot d\vec{a} \tag{5.17}$$

Using Gauss's law to express the surface integral of $\vec{E}$ in terms of the total enclosed charge *Q*, we obtain

$$I = \sigma \frac{Q}{\epsilon} \tag{5.18}$$

Now, the problem reduces to finding the relationship between the charge distribution and contact voltages. Using the Green's function, the potential resulting from any known charge distribution can be obtained. From the definition of Green's function (equation 5.1), the voltage distribution ϕ*(r)* is calculated by inverse transformation [24]

$$\phi(r) = \int_V \rho(r^{'}) G(r, r^{'})\, d^3 r^{'} \tag{5.19}$$

for a given charge distribution $\rho(r)$.

Since all contacts under consideration are surface contacts, all integrations will be performed on surfaces. A uniform charge distribution ρ is chosen over contact *j*. The potential at *r* due to Q_j is given by

$$\phi(r) = \frac{Q_j}{S_j} \int_{S_j} G(r, r^{'})\, ds_j \tag{5.20}$$

For sufficiently small contacts, the potential of a contact is defined as the average potential. The potential at contact *i* due to Q_j can now be written as

$$\bar{\phi_i} = \frac{Q_j}{S_i S_j} \int_{S_j} \int_{S_i} G\, ds_i\, ds_j \tag{5.21}$$

Using equation 5.21, for a given contact distribution, the elements p_{ij}, relating Q_j and $\bar{\phi}_i$ can be computed for all possible pairs of contacts, which is written in matrix form as

$$[\phi] = [P][Q] \tag{5.22}$$

The matrix [*P*] is called the "coefficient-of-potential" matrix. The inverse of this matrix [*c*] is called the "coefficient-of-induction" matrix and it gives the charge distribution for a voltage specification.

$$[Q] = [c][\phi] \tag{5.23}$$

Inserting equation 5.23 in equation 5.18, we get a relation between the currents vectors and voltage vectors.

$$[I] = \frac{\sigma}{\epsilon}[c][\phi] \tag{5.24}$$

The current flowing through the contact *i* can also be written as the sum of currents through all resistors R_{ij} between contact *i* and contact *j* and R_{ii} between contact *i* and ground plane.

$$I_i = \sum_{j \neq i} \frac{V_i - V_j}{R_{ij}} + \frac{V_i}{R_{ii}} \tag{5.25}$$

Comparing the last two equations gives the value of the resistors in the substrate between two contacts.

$$\begin{aligned} R_{ij} &= -\frac{\epsilon}{\sigma}\frac{1}{c_{ij}} \\ R_{ii} &= \frac{\epsilon}{\sigma}\frac{1}{\sum_j c_{ij}} \end{aligned} \tag{5.26}$$

A note on the implemention of Green's function is worth mentioning. The implementation of the Green's function in evaluating the resistances uses 2-D Discrete Cosine Transform. The DCT method was used in [21] and [22] to evaluate the parasitic capacitances and is adopted here. DCT of the Green's function is computed only once for a given substrate irrespective of the layout of contacts. The DCT is then used in table look-up approach for any given contact layout speeding up the computations of resistances dramatically.

5.3 Verification

3-D device simulations were performed to verify the Green's function derived earlier. Resistances between planar contacts placed on the surface of a substrate are extracted using Green's function and checked with the simulations. The 3-D device simulator TAURUS was used for this purpose. In the simulations, the backplane was not grounded since the substrate is grounded using bulk contacts from top in a conventional CMOS process. Since the backplane in 2-layer Green's function is grounded, the second layer in the 2-layer Green's function is made highly resistive. As mentioned in Chapter 4, the Green's function purpose is to identify scaling laws. In this section, some elementary guidlines will also be developed using the results from the simulations.

To begin with, parasitic resistances between three surface contacts were simulated. The substrate has 5E16 cm^{-3} p-type doping with dimensions $12\mu m \times 8\mu m \times 5\mu m$. The surface contacts layout and the parasitic resistors which are calculated are shown in figure 5.2 (a). Note that since the structure is symmetric, other parasitic resistors are identical to these two resistors R_{12} and R_{13}. The default values of layout parameters are spacing d = 0.5 μ m, width W = 1 μ m and length L = 4 μ m with substrate thickness t = 5 μ m. To validate the numerical values of the resistors and the scaling trends of the resistors predicted by Green's function, these parameters were changed individually. The two resistors R_{12} and R_{13} were extracted from Green's function and compared with simulations. Figure 5.2 shows the comparison between the theory and simulation. In all cases, agreement within 10 % is observed. More importantly, all the scaling trends are identical justifying the use of Green's function in deriving scaling laws without resorting to time consuming 3-D device simulations. As figure 5.2 indicates, the resistances increase with increasing spacing, decreasing width and decreasing length. Simulations were performed with horizontal contacts and all-around contacts also. The layout and the results are shown in figure 5.3, where a resistor R_i represents the resistance between the contact i and the substrate contact. It is interesting to observe that the resistance between the contact and substrate increases for deep contacts . For analyzing multi-finger devices, this indicates that the substrate resistances of only a few edge fingers might be sufficient. To validate this for vertical contacts also, layout in figure 5.4 was simulated, where the contact on the far left is treated as substrate contact. As seen from the results, resistance to the substrate contact increases dramatically for farther contacts. This again indicates that only the edge fingers are important for calculating resistances to the substrate contacts.

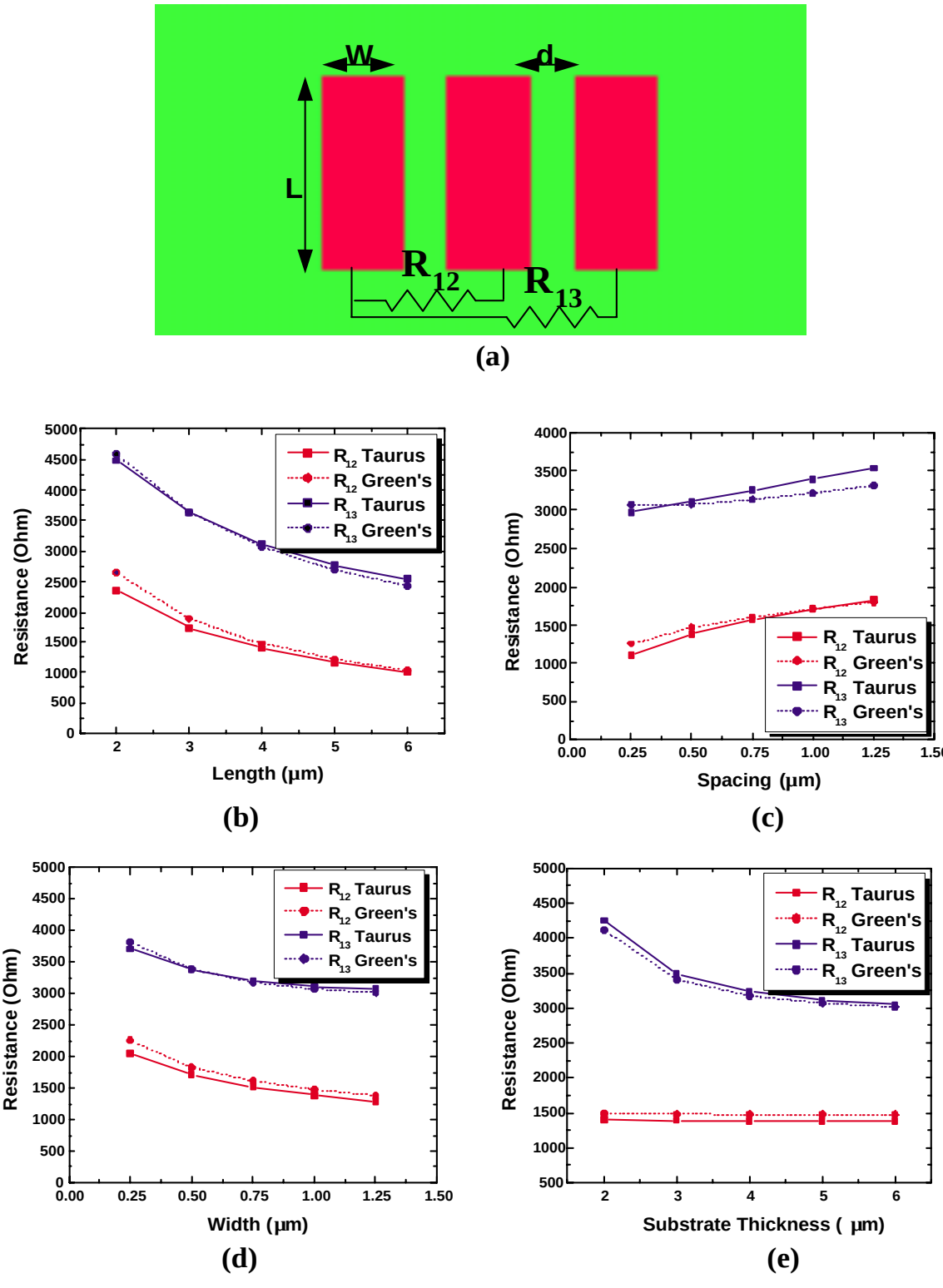

Figure 5.2: Layout of 3 surface contacts structure used to verify Green's Function

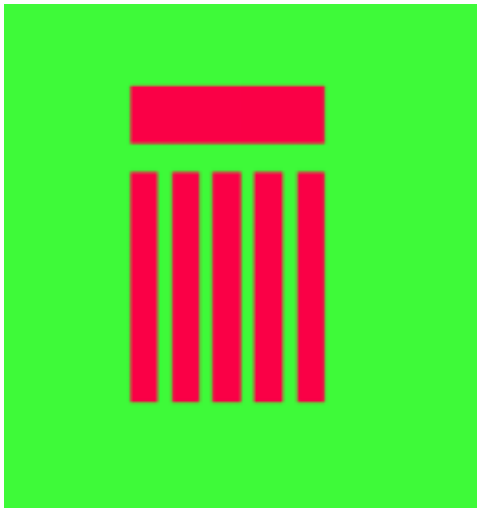

(a)

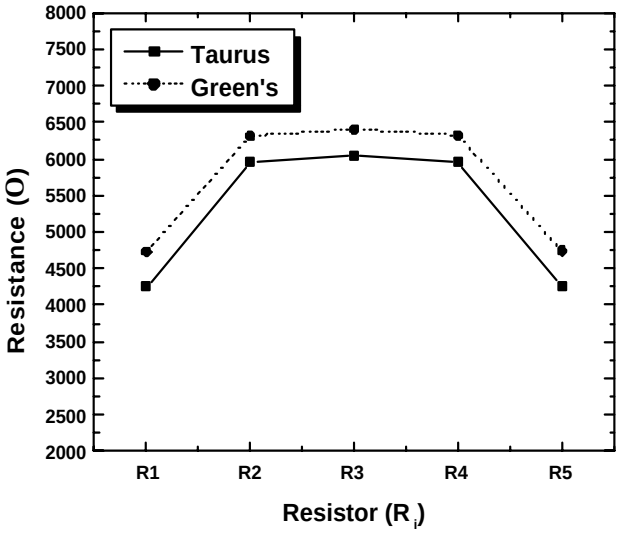

(b)

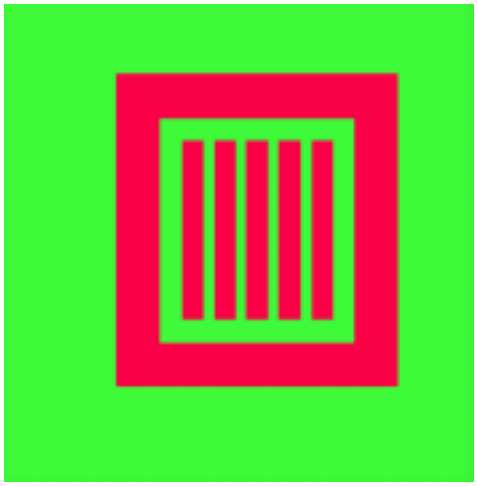

(c)

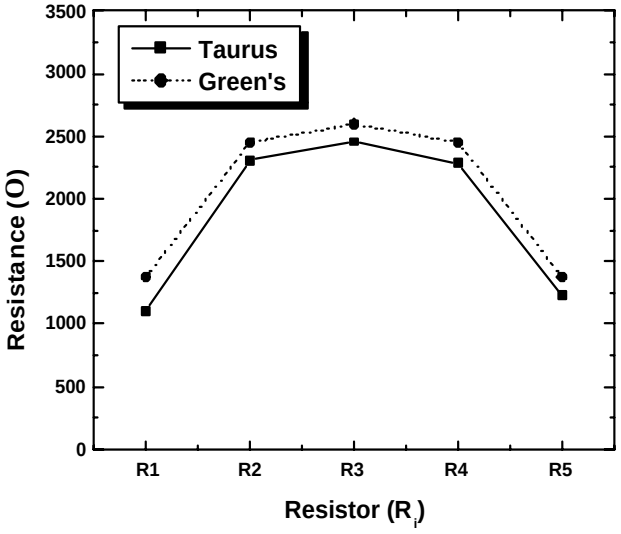

(d)

Figure 5.3: Surface contacts with Horizontal and All-around Substrate Contacts

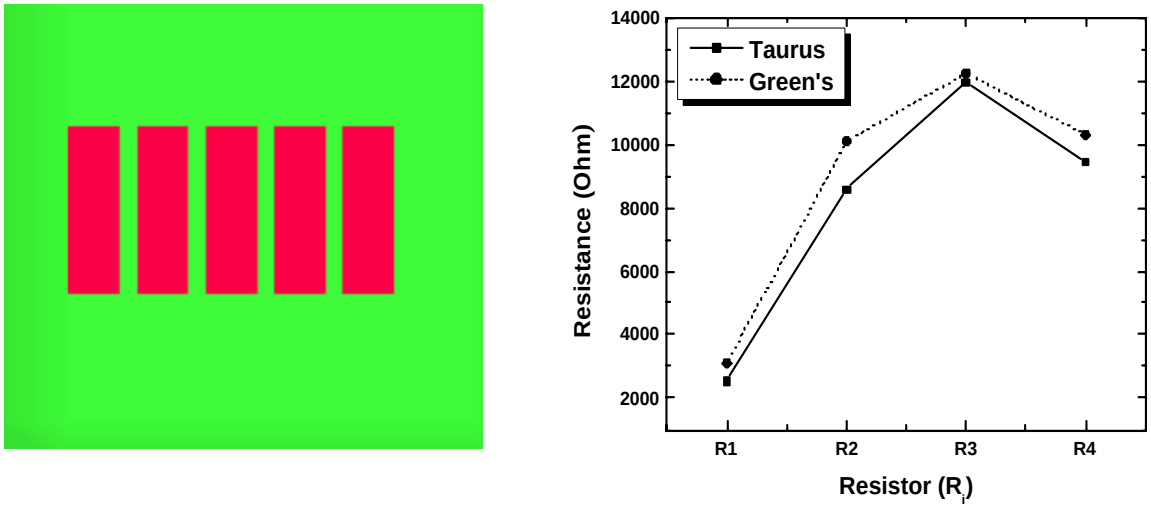

Figure 5.4: Surface contacts with Vertical Substrate Contact

It is observed that parasitic substrate resistance extraction by the use of Green's function shows good agreement with the simulation results. The trends obtained from Green's function match with the simulation trends. This analytical formulation can be used to generate the scaling parameters for the 5-R scalable network model.

Chapter 6

Conclusions

Substrate resistance has a considerable impact on the performance of high-frequency circuits and needs to be taken into account in circuit simulations. Three different configurations of the substrate resistance network 1-R ,3-R and 5-R resistive networks, were analyzed in detail. 2-D and 3-D simulations showed that 5-R network is required for predicting all the *Y*-parameters accurately. Due to increased computational time associated with the two additional nodes of 5-R substrate network, the 1-R network is suggested for use in cases where only Y_{22} is important. In order to make the 5-R resistor substrate network scalable, a model with 40 parameters was suggested initially. A careful consideration of the symmetries in the problem led to a scalable model with only 26 parameters for assymetric device and 20 parameters for symmetric device. To estimate the values of the network resistors, analytical equations using Green's function are developed. 3-D simulations showed that Green's function predicts the values of parasitic resistances in a substrate within 10% and gives identical scaling for the resistances. Green's function is thus shown to be appropriate to estimate the values of the scaling parameters of the 5-R substrate network.

6.1 Future work

MOSFETs with different kind of substrate layouts have been fabricated. *Y*-parameter data of the MOSFETs under off-state will be measured. The experimental data for the different substrate

contact layouts will be used to validate the 5-R network. The Green's function will be used to predict the scaling of the resistors. Default parameter values and reasonable range of values for the parameters will be calculated using the Green's function.

Bibliography

[1] L. E. Larson, "Integrated circuit technology options for RFIC's - Present status and future directions," *IEEE J. Solid-State Circuits*, vol. 33, pp. 387–399, March 1998.

[2] C. H. Diaz, D. D. Tang, and J. Sun, "CMOS technology for MS/RF SOC," *IEEE Trans. Electron Devices*, vol. 50, no. 3, pp. 557–566, March 2003.

[3] J. N. Burghartz *et al.*, "RF potential of a 0.18μm CMOS logic device technology," *IEEE Trans. Electron Devices*, vol. 47, no. 4, pp. 864–870, 2000.

[4] (2003, May) Bsim4.3.0 manual. [Online]. Available: http://www-device.eecs.berkeley.edu/ bsim3/bsim4.html

[5] M. Bucher, C. Lallement, C. Enz, F. Theodoloz, and F. Krummenacher. The EPFL-EKV MOSFET model, Version 2.6. [Online]. Available: http://legwww.epfl.ch/ekv/

[6] R. van Langevelde *et al.* (2001, Dec.) Mos11. [Online]. Available: http://www.semiconductors.philips.com/Philips_Models/mos_models/model11/

[7] C. C. Enz and Y. Cheng, "MOS Transistor modeling for RF IC design," *IEEE J. Solid-State Circuits*, vol. 35, pp. 186–201, Feb. 2000.

[8] W. Liu *et al.*, "R. F. MOSFET modeling accounting for distributed substrate and channel resistances with emphasis on the BSIM3v3 SPICE model," in *IEDM Tech. Dig.*, 1997, pp. 309–312.

[9] S. H.-M. Jen *et al.*, "Accurate modeling and parameter extraction for MOS transistors valid up to 10 GHz," *IEEE Trans. Electron Devices*, vol. 46, pp. 2217–2227, Nov. 1999.

[10] Y. Tsividis, *Operation and Modeling of the MOS Transistor*, 2nd ed. McGraw Hill, 1999.

[11] X. Jin *et al.*, "An Effective Gate Resistance model for CMOS RF and Noise modeling," *Techincal Digest of International Electron Devices Meeting*, pp. 961–964, Dec. 1998.

[12] D. M. Pozar, *Microwave Engineering*, 2nd ed. John-Wiley and Sons, Inc., 1997.

[13] M. Je, I. Kwon, H. Shin, and K. Lee, "MOSFET modeling and parameter extraction for RF IC's," *International Journal of High Speed Electronics and Systems*, vol. 11, no. 4, pp. 953–1006, 2001.

[14] Y. Cheng and M. Matloubian, "On the high-frequency characteristics of substrate resistance in RF MOSFETs," *IEEE Electron Device Lett.*, vol. 21, no. 12, pp. 604–606, Dec. 2000.

[15] Y. Cheng *et al.*, "Parameter extraction of accurate and scalable substrate resistance components in RF MOSFETs," *IEEE Electron Device Lett.*, vol. 23, no. 4, pp. 221–223, Apr. 2002.

[16] J. Han, M. Je, and H. Shin, "A simple and accurate method for extracting substrate resistance of RF MOSFETs," *IEEE Electron Device Lett.*, vol. 23, no. 7, pp. 434–436, July 2002.

[17] J. Han *et al.*, "A scalable model for the substrate resistance in Multi-Finger RF MOSFETs," *IEEE Trans. Microwave Theory Tech.*, vol. 3, pp. 2105–2108, June 2003.

[18] Y. Cheng, "MOSFET modeling for RF design," *International Journal of High Speed Electronics and Systems*, vol. 11, no. 4, pp. 121–186, 2001.

[19] S. Lee, C. Kim, and H. K. Yu, "A RF MOSFET SPICE model with a new substrate network," in *Proc. of RAWCON 2000 Radio and Wireless Conference*, Denver, Colarado, USA, Sept. 2000, pp. 227–230.

[20] N. K. Verghese, D. J. Allstot, and S. Masui, "Rapid simulations of substrate coupling in mixed-mode ICs," in *Proc. IEEE Custom Integrated Circuits Conference*, May 1993, pp. 18.3.1–18.3.4.

[21] R. Gharpurey and R. G. Meyer, "Modeling and analysis of substrate coupling in integrated circuits," *IEEE J. Solid-State Circuits*, vol. 31, no. 3, pp. 344–352, March 1996.

[22] A. M. Niknejad, R. Gharpurey, and R. G. Meyer, "Numerically stable green function for modeling and analysis of substrate coupling in integrated circuits," *IEEE Trans. Computer-Aided Design*, vol. 17, no. 4, pp. 305–315, Apr. 1998.

[23] S. Ramo, J. R. Whinnery, and T. V. Duzer, *Fields and Waves in Comunication Electronics*, 2nd ed. New York, USA: John Wiley and Sons, Inc., 1984.

[24] G. Barton, *Elements of Green's Functions and Propogation*. New York, USA: Oxford University Press, 1989.

Appendix A

Y-parameters for 1-R Network

The 1-R resistor network is shown in Figure A.1. The 2 ports for *Y*-parameter analysis are Gate-Source (Port 1) and Drain-Source (Port 2) with the bulk terminal grounded. To calculate Y_{11} and Y_{21}, Port 2 is grounded and the current through gate and drain are measured. Figure A.2 (a) shows the equivalent circuit to evaluate Y_{11} and Y_{21}. From Figure A.2(a),

$$\begin{aligned} Y_{11} &= \frac{I_1}{V_1}\Big|_{V_2=0} = \frac{I_g}{V_{gs}}\Big|_{V_{ds}=0} \\ &= j\omega C_{gd} + j\omega C_{gs} + Y' \end{aligned} \tag{A.1}$$

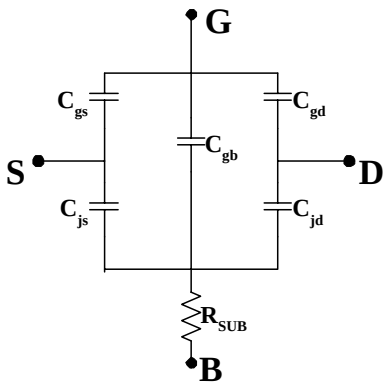

Figure A.1: One Resistor Substrate Network

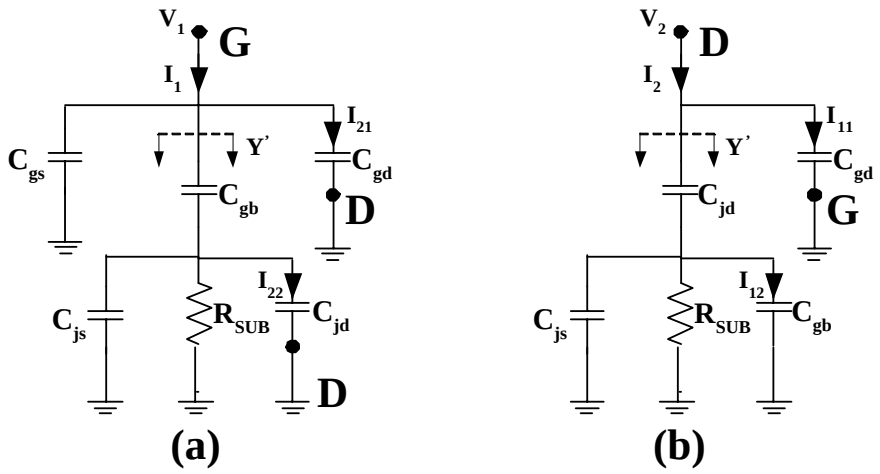

Figure A.2: Equivalent Circuits for calculating (a) Y_{11}, Y_{21} and (b) Y_{22}, Y_{12} for 1-R network

Define $C_j = C_{js} + C_{jd}$. From Figure A.2 (a), $Y^{'}$ can be shown to be

$$Y^{'} = \frac{j\omega C_{gb}\,[\frac{1}{R_{SUB}} + j\omega C_j]}{j\omega C_{gb} + [\frac{1}{R_{SUB}} + j\omega C_j]} \tag{A.2}$$

Using equations A.1 and A.2,

$$\begin{aligned} Im[Y_{11}] &= \omega C_{gd} + \omega C_{gs} + \frac{\omega C_{gb} + \omega^3 R_{SUB}^2 C_{gb} C_j\,[C_{gb} + C_j]}{1 + \omega^2 R_{SUB}^2\,[C_{gb} + C_j]^2} \qquad \text{(A.3)} \\ Re[Y_{11}] &= \frac{\omega^2 R_{SUB}\,C_{gb}^2}{1 + \omega^2 R_{SUB}^2\,[C_{gb} + C_j]^2} \end{aligned}$$

Under low frequency approximation,

$$\begin{aligned} Im[Y_{11}] &= \omega(C_{gd} + C_{gs} + C_{gb}) \qquad \text{(A.4)} \\ Re[Y_{11}] &= \omega^2 R_{SUB} C_{gb}^2 \end{aligned}$$

Using the equivalent circuit Figure A.2 (a) to calculate Y_{21}

$$\begin{aligned} Y_{21} &= \frac{I_2}{V_1}\Big|_{V_2=0} = \frac{I_d}{V_{gs}}\Big|_{V_{ds}=0} \qquad \text{(A.5)} \\ &= -\frac{I_{21} + I_{22}}{V_1} \end{aligned}$$

From Figure A.2 (a), it can be seen that

$$\frac{I_{21}}{V_1} = j\omega C_{gd} \tag{A.6}$$

$$\begin{aligned} \frac{I_{22}}{V_1} &= \left[\frac{j\omega C_{jd}}{\frac{1}{R_{SUB}} + j\omega C_j}\right] \frac{I^{'}}{V_1} \qquad \text{(A.7)} \\ &= \left[\frac{j\omega C_{jd}}{\frac{1}{R_{SUB}} + j\omega C_j}\right] Y^{'} \end{aligned}$$

Using equations A.2, A.5, A.6 and A.7,

$$\begin{aligned} Im[Y_{21}] &= -j\omega C_{gd} - \frac{\omega^3 R_{SUB}^2 C_{jd} C_{gb} \left[C_{gb} + C_j\right]}{1 + \omega^2 R_{SUB}^2 \left[C_{gb} + C_j\right]^2} \\ Re[Y_{21}] &= \frac{\omega^2 R_{SUB} C_{jd} C_{gb}}{1 + \omega^2 R_{SUB}^2 \left[C_{gb} + C_j\right]^2} \end{aligned} \tag{A.8}$$

Under low frequency approximatopn,

$$\begin{aligned} Im[Y_{21}] &= -\omega C_{gd} \\ Re[Y_{21}] &= \omega^2 R_{SUB} C_{gb} C_{jd} \end{aligned} \tag{A.9}$$

To calculate Y_{22} and Y_{12}, Port 1 is grounded and the current through drain and gate are measured. Figure A.2 b shows the equivalent circuit to evaluate Y_{22} and Y_{12}. A careful look at Figure A.2 (a) and Figure A.2 (b) reveals that they are identical when C_{gs} is removed and following interchanges are made.

$$\begin{aligned} C_{jd} &\longrightarrow C_{gb} \\ C_{gb} &\longrightarrow C_{jd} \end{aligned} \tag{A.10}$$

Using this, one can simply write Y_{22} and Y_{12} from equations A.3 and A.8 as

$$\begin{aligned} Im[Y_{22}] &= \omega C_{gd} + \frac{\omega C_{gd} + \omega^3 R_{SUB}^2 C_{jd} \left[C_{gb} + C_{js}\right] \left[C_{gb} + C_j\right]}{1 + \omega^2 R_{SUB}^2 \left[C_{gb} + C_j\right]^2} \\ Re[Y_{22}] &= \frac{\omega^2 R_{SUB}\, C_{jd}^2}{1 + \omega^2 R_{SUB}^2 \left[C_{gb} + C_j\right]^2} \end{aligned} \tag{A.11}$$

$$\begin{aligned} Im[Y_{12}] &= -j\omega C_{gd} - \frac{\omega^3 R_{SUB}^2 C_{jd} C_{gb} \left[C_{gb} + C_j\right]}{1 + \omega^2 R_{SUB}^2 \left[C_{gb} + C_j\right]^2} \\ Re[Y_{12}] &= \frac{\omega^2 R_{SUB} C_{jd} C_{gb}}{1 + \omega^2 R_{SUB}^2 \left[C_{gb} + C_j\right]^2} \end{aligned} \tag{A.12}$$

Under low frequency approximations,

$$Im[Y_{22}] = \omega(C_{gd} + C_{jd}) \tag{A.13}$$

$$Re[Y_{22}] = \omega^2 R_{SUB} C_{jd}^2$$

$$Im[Y_{12}] = -\omega C_{gd} \tag{A.14}$$

$$Re[Y_{12}] = \omega^2 R_{SUB} C_{jd} C_{gb}$$

Appendix B

Y-parameters for 3-R Network

The 3-R resistor network is shown in Figure B.1. The two ports for *Y*-parameter analysis are Gate-Source (Port 1) and Drain-Source (Port 2) with the bulk terminal grounded. Since all the definitions are the same as the 1-R network, only the equivalent circuits and the important equations in the equivalent circuit analysis will be shown.

To calculate Y_{11}, from the equivalent circuit Figure B.2 (a)

$$\begin{aligned} Y_{11} &= \frac{I_1}{V_1}\Big|_{V_2=0} \\ Y_{11} &= j\omega C_{gs} + j\omega C_{gd} + Y_1 \end{aligned} \tag{B.1}$$

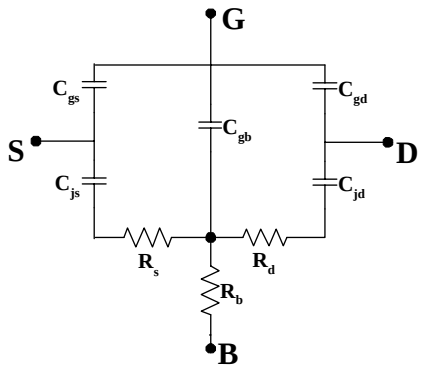

Figure B.1: Three Resistor Substrate Network

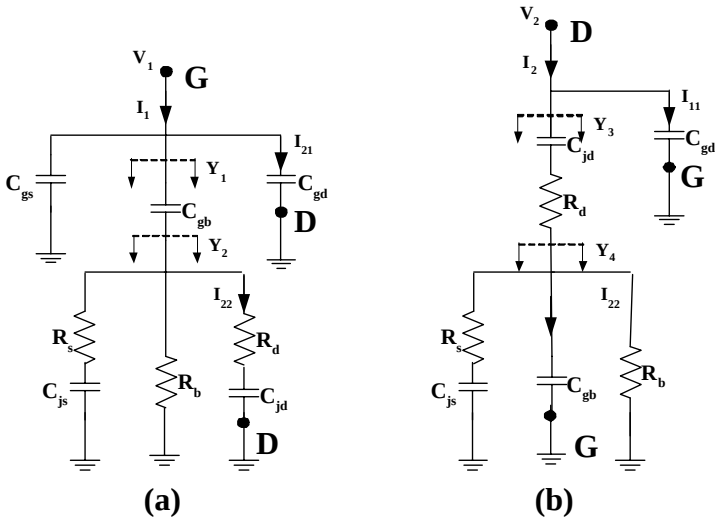

Figure B.2: Equivalent Circuits for calculating (a) Y_{11}, Y_{21} and (b) Y_{22}, Y_{12} for 3-R network

where

$$Y_1 = \frac{j\omega C_{gb} Y_2}{j\omega C_{gb} + Y_2} \tag{B.2}$$

$$Y_2 = \frac{1}{R_b} + \frac{j\omega C_{js}}{1 + j\omega R_s C_{js}} + \frac{j\omega C_{jd}}{1 + j\omega R_d C_{jd}} \tag{B.3}$$

Using equations B.1, B.2 and B.3, Y_{11} can be calculated. Under low frequency approximation,

$$Im[Y_{11}] = \omega(C_{gd} + C_{gs} + C_{gb}) \tag{B.4}$$

$$Re[Y_{11}] = \omega^2 R_b C_{gb}^2 \tag{B.5}$$

To calculate Y_{21}, from the equivalent circuit Figure B.2 (a)

$$Y_{21} = \frac{I_2}{V_1}\Big|_{V_2=0} \tag{B.6}$$

$$Y_{21} = -\frac{I_{21} + I_{22}}{V_1}$$

where

$$\frac{I_{21}}{V_1} = j\omega C_{gd} \tag{B.7}$$

$$\frac{I_{22}}{V_1} = Y_1 \frac{\frac{1}{\frac{1}{R_d} + j\omega C_{jd}}}{Y_2} \tag{B.8}$$

Y_{21} is calculated from equations B.6, B.7 and B.8. Under low frequency approximations,

$$Im[Y_{21}] = -\omega C_{gd} \quad \text{(B.9)}$$

$$Re[Y_{21}] = \omega^2 R_b C_{gb} C_{jd} \quad \text{(B.10)}$$

To calculate Y_{22}, from the equivalent circuit Figure B.2 (b)

$$Y_{22} = \frac{I_2}{V_2}\Big|_{V_1=0} \quad \text{(B.11)}$$

$$Y_{22} = j\omega C_{gd} + Y_3$$

where

$$Y_3 = \frac{1}{\frac{1}{j\omega C_{jd}} + R_d + \frac{1}{Y_4}} \quad \text{(B.12)}$$

$$Y_4 = \frac{1}{R_b} + j\omega C_{gb} + \frac{j\omega C_{js}}{1 + j\omega R_s C_{js}} \quad \text{(B.13)}$$

Using equations B.11, B.12 and B.13 , Y_{22} can be calculated. Under low frequency approximation,

$$Im[Y_{22}] = \omega(C_{gd} + C_{jd}) \quad \text{(B.14)}$$

$$Re[Y_{22}] = \omega^2 (R_b + R_d) C_{gb}^2 \quad \text{(B.15)}$$

To calculate Y_{12}, from the equivalent circuit Figure B.2 (b)

$$Y_{12} = \frac{I_1}{V_2}\Big|_{V_1=0} \quad \text{(B.16)}$$

$$= -\frac{I_{11} + I_{12}}{V_2}$$

where

$$\frac{I_{11}}{V_2} = j\omega C_{gd} \quad \text{(B.17)}$$

$$\frac{I_{12}}{V_2} = \frac{Y_3}{Y_4}\, j\omega C_{gb} \quad \text{(B.18)}$$

Y_{12} is calculated from equations B.16, B.17 and B.18. Under low frequency approximations,

$$Im[Y_{12}] = -\omega C_{gd} \quad \text{(B.19)}$$

$$Re[Y_{12}] = \omega^2 R_b C_{jd} C_{gb} \quad \text{(B.20)}$$

Appendix C

Y-parameters for 5-R Network

The 5-R resistor network is shown in Figure C.1. The two ports for *Y*-parameter analysis are Gate-Source (Port 1) and Drain-Source (Port 2) with the bulk terminal grounded. Since all the definitions are the same as the 1-R network, only the equivalent circuits and the important equations in the equivalent circuit analysis will be shown.

To calculate Y_{11}, from the equivalent circuit Figure C.2 (a)

$$\begin{aligned} Y_{11} &= \frac{I_1}{V_1}\Big|_{V_2=0} \\ Y_{11} &= j\omega C_{gs} + j\omega C_{gd} + \frac{1}{Z} \end{aligned} \tag{C.1}$$

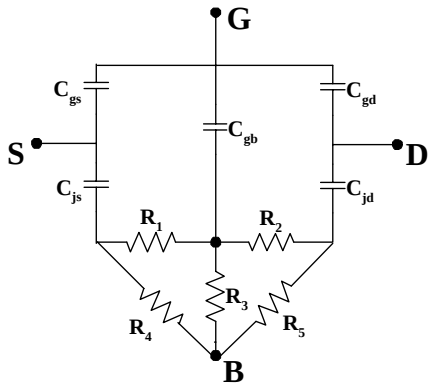

Figure C.1: Five Resistor Substrate Network

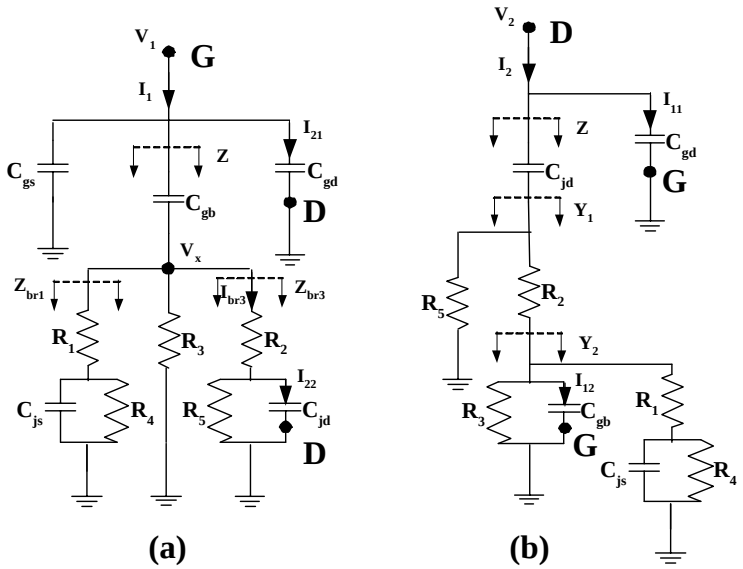

Figure C.2: Equivalent Circuits for calculating (a) Y_{11}, Y_{21} and (b) Y_{22}, Y_{12} for 5-R network

where

$$Z = \frac{1}{j\omega C_{gb}} + \frac{1}{\frac{1}{Z_{br1}} + \frac{1}{R_3} + \frac{1}{Z_{br3}}} \tag{C.2}$$

$$Z_{br1} = R_1 + \frac{1}{j\omega C_{js} + \frac{1}{R_4}} \tag{C.3}$$

$$Z_{br3} = R_2 + \frac{1}{j\omega C_{jd} + \frac{1}{R_5}} \tag{C.4}$$

Using equations C.1 to C.4, Y_{11} can be calculated. Under low frequency approximation,

$$Im[Y_{11}] = \omega(C_{gd} + C_{gs} + C_{gb}) \tag{C.5}$$

$$Re[Y_{11}] = \omega^2 C_{gb}^2 \left[R_3||(R_1 + R_4)||(R_2 + R_5)\right] \tag{C.6}$$

To calculate Y_{21}, from the equivalent circuit Figure C.2 (a)

$$Y_{21} = \frac{I_2}{V_1}\Big|_{V_2=0} \tag{C.7}$$

$$Y_{21} = -\frac{I_{21} + I_{22}}{V_1}$$

where

$$I_{21} = j\omega C_{gd} V_1 \tag{C.8}$$

$$I_{22} = \frac{R_5}{R_5 + \frac{1}{j\omega C_{jd}}} I_{br3} \tag{C.9}$$

$$I_{br3} = \frac{V_x}{Z_{br3}} \tag{C.10}$$

$$V_x = V_1 \left[1 - \frac{1}{Z} \frac{1}{j\omega C_{gb}}\right] \tag{C.11}$$

Y_{21} is calculated from equations C.7 to C.11. Under low frequency approximations,

$$Im[Y_{21}] = -\omega C_{gd} \tag{C.12}$$

$$Re[Y_{21}] = \omega^2 C_{jd} C_{gb} \overbrace{\left[\frac{R_5}{R_5 + R_2}\right] [R_3||(R_1 + R_4)||(R_2 + R_5)]} = \omega^2 C_{jd} C_{gb} R12 \tag{C.13}$$

To calculate Y_{22}, from the equivalent circuit Figure C.2 (b)

$$Y_{22} = \frac{I_2}{V_2}\Big|_{V_1=0} \tag{C.14}$$

$$Y_{22} = j\omega C_{gd} + \frac{1}{Z}$$

where

$$Z = \frac{1}{j\omega C_{jd} + \frac{1}{Y_1}} \tag{C.15}$$

$$Y_1 = \frac{1}{R_5} + \frac{1}{R_2 + \frac{1}{Y_2}} \tag{C.16}$$

$$Y_2 = \frac{1}{R_3} + j\omega C_{gb} + \frac{1}{R_1 + \frac{1}{j\omega C_{js} + \frac{1}{R_4}}} \tag{C.17}$$

Using equations C.14 to C.17, Y_{22} can be calculated. Under low frequency approximation,

$$Im[Y_{22}] = \omega(C_{gd} + C_{jd}) \tag{C.18}$$

$$Re[Y_{22}] = \omega^2 C_{jd}^2 \overbrace{R12(1 + \frac{R_2}{R_3} + \frac{R_2}{R_1 + R_4})} = \omega^2 C_{jd}^2 R22 \tag{C.19}$$